Defence Science Journal, Vol. 66, No. 4, July 2016, pp. 403-412, DOI : 10.14429/dsj.66.10215
© 2016, DESIDOC

RESEARCH PAPER

Effect of Fe on the Martensitic Transition, Magnetic and Magnetocaloric Properties in Ni-Mn-In Melt-spun Ribbons

D.M. Raj kumar[#,*], N.V. Rama Rao[#], S. Esakki Muthu[$], S. Arumugam[$], M. Manivel Raja[#], and K.G. Suresh[!]

[#]*Advanced Magnetics Group, Defence Metallurgical Research Laboratory, Hyderabad – 500 058, India*
[$]*Centre for High Pressure Research, School of Physics, Bharathidasan University, Trichy -600 026, India*
[!]*Department of Physics, Indian Institute of Technology Bombay, Mumbai – 400 076, India*
[*]*E-mail: rajkumardmrl@gmail.com*

ABSTRACT

The effect of Fe on the martensitic transitions, magnetic and inverse magnetocaloric effect in $Ni_{47}Mn_{40-x}Fe_xIn_{13}$ ribbons (x = 1, 2, 3, and 5) has been investigated. All the ribbon compositions under study have shown the presence of austenite phase at room temperature. The variation of martensitic transition with the increase in Fe-content is non-monotonic. The thermal hysteresis of the martensitic transition increased with the increase in Fe-content. The martensitic transitions shifted to lower temperatures in the presence of high magnetic fields. A maximum magnetic entropy change (ΔS_M) of 50 $Jkg^{-1}K^{-1}$ has been achieved in the $Ni_{47}Mn_{38}Fe_2In_{13}$ (x = 1) ribbon at 282 K for an applied field of 5 T.

Keywords: Thermo-magnetic behaviour, magnetocaloric effect, martensitic transition

1. INTRODUCTION

The Ni-Mn-Y (Y = Ga, In, Sn, and Sb) based ferromagnetic Heusler alloys display first order martensitic transitions from cubic to tetragonal or orthorhombic structure upon cooling. Associated with the martensitic transition observed in these alloys several important functional properties such as shape memory effect, inverse magnetocaloric effect and magnetoresistance have been reported[1-3]. The martensitic and magnetic transitions in these alloys are composition dependent as they are highly sensitive to the valence electron concentration per atom (e/a) and Mn-Mn interatomic distances[4,5]. In the case of Indium (In) containing alloys, a large inverse magnetocaloric effect (IMCE) in polycrystalline state and significant magnetic field induced strain (MFIS) in single crystals have been reported[6,7]. Recently rapid quenching or melt spinning technique was attempted in various systems such as Ni-Fe-Ga, Ni-Mn-Y (Y = In, Al, Sn, and Ga) alloys[8-11]. The melt spinning technique has the advantage of producing strong textured polycrystalline ribbons. In the case of magnetic refrigeration applications the use of refrigerant materials in the form of thin films or ribbons can optimize the heat transfer between the working body and the heat-exchange fluid. Additional advantage of melt spun ribbons is that the thin ribbons reduces the eddy current losses and can be utilised at high frequencies. In the recent past, off-stoichiometric Ni-Mn-In ribbons has gained lot of interest due to their intriguing martensitic phase transitions, microstructure, associated magnetic, magnetocaloric properties[12-17]. In the present study, off-stoichiometric $Ni_{47}Mn_{40}In_{13}$ ribbon composition which reported a large magnetic entropy change of 32 J/kg-K at RT was chosen and Mn was partially substituted by Fe[18]. The objective of this work is to understand the effect of Fe on the martensitic transitions, magnetic and magnetocaloric properties in Ni-Mn-In ribbons. Hence, $Ni_{47}Mn_{40-x}Fe_xIn_{13}$ (x = 1, 2, 3, and 5) ribbons were prepared through melt spinning route and studied.

Received : 21 March 2016, Revised : 13 May 2016
Accepted : 10 June 2016, Online published : 28 June 2016

2. EXPERIMENTAL WORK

Four Ni-Mn(Fe)-In alloys were prepared by arc-melting pure metals in an argon atmosphere. Subsequently they were induction melted in a quartz tube and ejected with a 1 bar pressure difference onto a copper wheel rotating at a surface velocity of 17 m/s. The process was carried out in argon environment. As-quenched ribbons were 1.5 mm - 2 mm wide, 5 mm -18 mm long and 40 µm - 45 µm thick. As-spun ribbons were annealed at 850 °C for 30 min in vacuum and quenched to room temperature using Argon gas. The crystal structure of the constituent phases were examined using an X-ray diffractometer (PHILIPS3121, Cu-K_α λ = 1.54058 Å). The compositions of the ribbons were determined by energy dispersive x-ray spectroscopy (EDX) and were found to be close to the nominal composition. The phase transitions between the martensite and austenite phases were determined by differential scanning calorimetry (DSC) with a cooling/heating rate of 20 K/min. The magnetisation measurements were performed by means of vibrating sample magnetometer in physical property measurement system (PPMS, Quantum design P525) in the temperature range of 4 K - 320 K. The sample was initially cooled in the absence of an external magnetic field and the data was collected on warming by applying an external magnetic field of 0.05 T termed as zero field cooled (ZFC) M(T) curve. Subsequently, the data was recorded upon cooling termed as field cooled (FC) M(T) curve without removing the applied field. The isothermal magnetisation curves were recorded for both increasing and decreasing fields for a maximum field of 5 T in the vicinity of structural transitions.

3. RESULTS AND DISCUSSION

3.1 Structural Analysis

Figure 1 (a)-(d) shows the x-ray diffraction patterns of $Ni_{47}Mn_{40-x}Fe_xIn_{13}$ ribbons recorded at room temperature (RT). The X-ray diffraction patterns of the x = 2 and 3 ribbons have been re-recorded using a step scan of 0.01° for a time interval of 4 s in the 2θ range of 30°-52.5° and 62.5°-80° (Fig .1(e) and 1(f)). The x = 1, 2, and 5 ribbons revealed the presence of cubic $L2_1$ structure (austenite phase) at RT and no secondary phases were detected. This suggests that the martensitic transitions of these ribbons are below RT. In the case of x = 3 ribbon, step scan revealed the presence of a small volume fraction of the martensite along with major austenite phase which suggests that the martensite transition of the x = 3 ribbon is around RT. The lattice parameters of the austenite phase in x = 1, 2, 3, and 5 ribbons are 0.5992 nm, 0.5987 nm, 0.5982 nm, and 0.5979 nm respectively. The partial substitution of Fe for Mn makes the lattice shrink because of the smaller atomic radius of Fe than that of Mn. Y. Feng et al. reported the presence of γ secondary phase in the $Ni_{50}Mn_{34}In_{16-y}Fe_y$ (y = 0-8) alloys for[19] y ≥ 5. This was found to be due to the solid solubility limit of Fe in Ni-Mn-In alloys about 4 at. per cent. In the current ribbon series, no secondary phases were observed after doping Fe up to 5 at. per cent. This suggests that melt spinning technique has enhanced the solubility limit.

3.2 Phase Transformations

The cyclic DSC thermograms of $Ni_{47}Mn_{40-x}Fe_xIn_{13}$ melt spun ribbons (Fig. 2) display an exothermic peak for the phase transformation from austenite to martensite (A→M) upon cooling and reverses (M→A) as an endothermic peak upon heating. The values of M_s, M_f, A_s and A_f are given in Table 1. Evidently, these ribbons display both first order structural transformation associated with martensitic transition and a second order magnetic transition (slope change in base line) corresponding to the Curie temperature of the austenite phase (T_C^A). All the ribbons except x = 2 show one peak which corresponds to the structural transition ($M \rightarrow A$) followed by a magnetic transition of the austenite phase (T_C^A) upon heating. The x = 2 ribbon shows two peaks with significant thermal hysteresis upon heating and cooling suggesting the presence of two structural transitions. In the cooling run, the first exothermic peak corresponds to the premartensitic transition (PMT) ~ 294 K followed by a martensitic transition ~ 255 K. This PMT is believed to be the precursor for the martensitic transition. The magneto-elastic coupling was found to play an important role for the occurrence of this precursor effect. Very recently, it was reported that PMT was observed in Sn-doped Ni_2MnGa at the Ga site up to 5 at per cent[20]. This suggests that the presence of Fe influences the magneto-elastic coupling in Ni-Mn-In ribbons. Except in the x = 2 ribbon sample, PMT was not observed in other compositions which could be due to other factors suppressing PMT which needs further

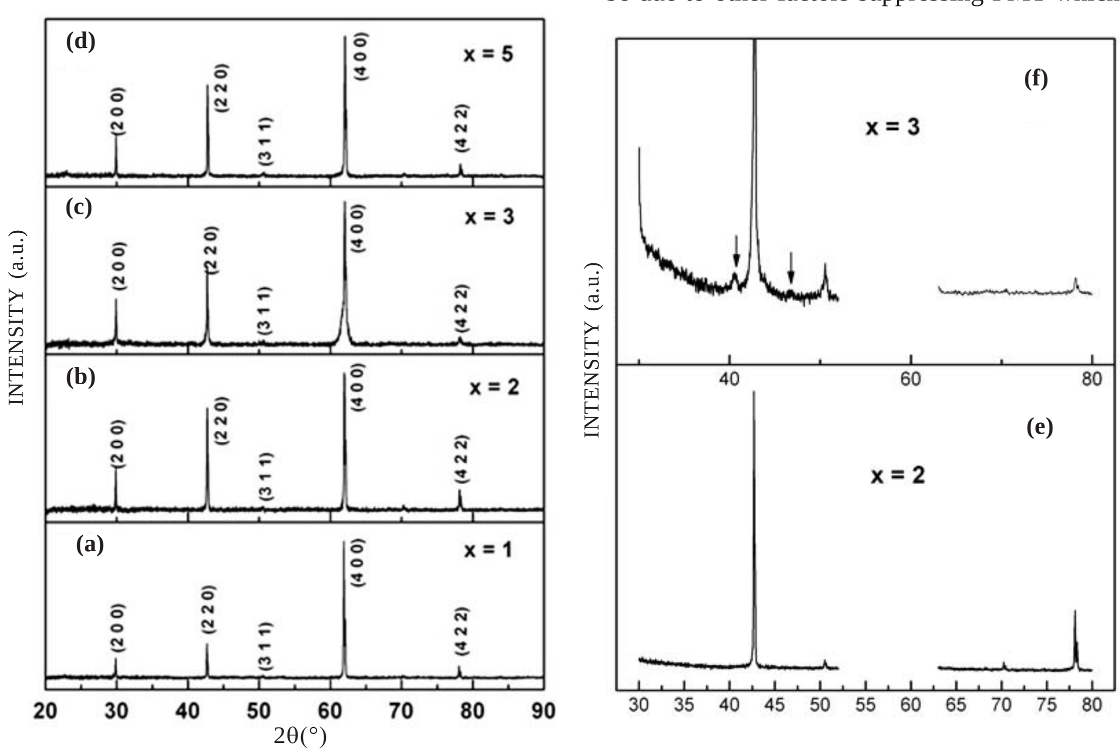

Figure 1. X-ray diffraction patterns for $Ni_{47}Mn_{40-x}Fe_xIn_{13}$ (a) x = 1 (b) x = 2 (c) x = 3 (d) x = 5 (e) and (f) slow scans of x = 2 and 3 ribbons in selected ranges of 2θ respectively at RT.

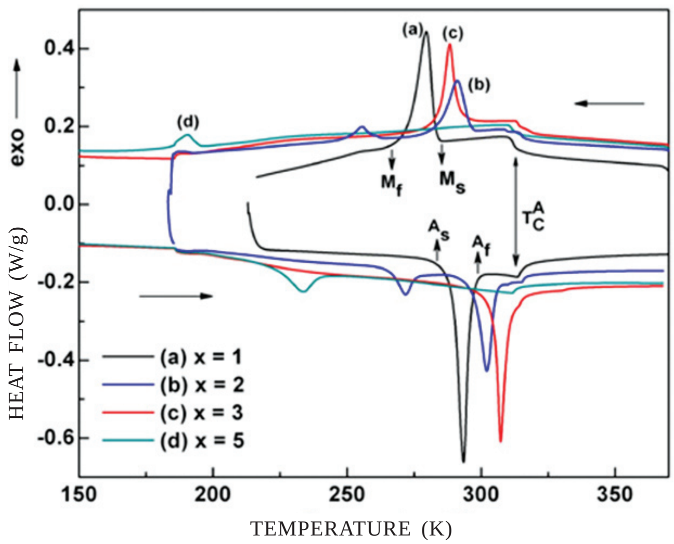

Figure 2. DSC curves for $Ni_{47}Mn_{40-x}Fe_xIn_{13}$ (x = 1, 2, 3, 5) ribbons upon heating and cooling at a rate of 20 K/min.

understanding. It was also found that the thermal hysteresis increases with the increase in Fe-content. For the x = 1 ribbon, T_M was around 292 K and for x = 2 ribbon, the T_M lowered to 270 K. In the case of x =3 ribbon, the T_M increased to 303 K and again drastically lowered to 218 K for the x = 5 ribbon. The X-ray analysis of the x = 3 ribbon (slow scan) revealed the presence of low volume fraction of the martensite phase along with major austenite phase at RT. The DSC results support the XRD studies. It can be seen that the variation of T_M with the increase in Fe concentration is non-monotonic.

Table 1. Values of the austenite start temperature (A_s), austenite finish temperature (A_f), martensite start temperature (M_s), martensite finish temperature (M_f), Martensitic transition temperature (T_M), Curie temperature (T_C^A), enthalpy (ΔH_{ep}, average of the values upon heating and cooling), thermal entropy change (ΔS_T) and valence electron concentration per atom (e/a)

x	Method	Transformation temperatures (K)				T_M^* (K)	T_C^A (K)	ΔH_{ep} (J/g)	ΔS_T (J/kg-K)	e/a
		A_s	A_f	M_s	M_f					
1	M(T)	286	293	290	279	291	311	6.6	22.8	7.90
	DSC	288	297	285	272	291	314			
2	M(T)	263	281	262	248	270	309	0.8	2.9	7.91
	DSC	264	278	262	246	270	310			
3	M(T)	305	315	294	283	304	317	5.5	18.2	7.92
	DSC	305	314	292	284	303	314			
5	M(T)	226	247	208	176	227	313	1.3	5.7	7.94
	DSC	224	241	195	183	218	312			

$^*T_M [= ½(M_s+A_f)]$

In general, the compositional dependence of martensitic transition (T_M) is related to the valence electron concentration (e/a). In view of that, a linear change of T_M with composition is expected due to the monotonic change in the number of valence electrons which has been well reported in various analogous systems[21-23]. However, in the present case the variation of T_M with e/a was observed to be non-linear. This suggests that additional parameters other than electron concentration could affect phase stability. The non-monotonous nature of T_M as a function of e/a in the present study suggests that the effect of alloying is not just a change in the Fermi level, but the addition of Fe could also modify to some extent the orbital hybridisation and bonding. The changes in hybridisation and related volume effects were reported for Ni_2MnGa with substitutions[20,24]. Hence, a simple choice of e/a can only be a guideline for examining systematic changes within a single alloy system and is not universal for related quaternary systems. It was reported that the dopant would create negative/positive pressure due to expansion/contraction of lattice volume[25]. Such pressure effect can dominate over the effect related to e/a. It has been observed that hydrostatic pressure can enhance the MT in many Ni-Mn based alloys. In the current study, similar effects are possible with the Fe substitution in Ni-Mn-In ribbons. Hence, the influence of multiple factors like composition (or e/a), pressure (or volume) and atomic disorder led to the observed complex behaviour of T_M with Fe-content.

The ZFC and FC magnetisation measurements of $Ni_{47}Mn_{40-x}Fe_xIn_{13}$ ribbons carried out as a function of temperature in a field of 0.05 T (500 Oe) are as shown in Fig. 3. All the ribbons (x = 1-5) show Curie transitions of the martensite phases (T_C^M) at low temperatures and splitting between the FC and ZFC curves below T_C^M. The T_C^M of the x = 1, 2, and 3 ribbons were observed at around same temperature 165 K whereas the x = 5 ribbon's T_C^M was found to be ~ 200 K. The T_C^M of the x = 5 ribbon could not be determined accurately from the ZFC and FC curves as it was overlapping with its martensitic phase transition. The T_C^M of the base composition $Ni_{47}Mn_{40}In_{13}$ ribbon was ~ 120 K and it has increased to 165 K for substituting Fe up to 3 at.% for Mn. With further increase in Fe (5 at. %), T_C^M has increased to ~ 200 K. This suggests that the presence of Fe enhances the ferromagnetic exchange interactions in the martensite phase in this series. At low temperatures (T<100 K), another transition T_{EB}, called exchange bias blocking temperature, is observed in the ZFC curves. The observation of T_{EB} and splitting of FC and ZFC curves suggest that there exist antiferromagnetic (AFM) and ferromagnetic (FM) interactions in these ribbons at low temperatures. The exchange bias blocking temperatures (T_{EB}) of the x = 1, 2, 3, and 5 ribbons are 55 K, 25 K, 51 K, and ~ 7 K respectively. The variation in the T_{EB} values with the increase in Fe-content was non-monotonous, but the general trend (except for the x = 3 ribbon) appears to be decreasing with increase in Fe-content. This may be attributed to the decrease in the FM-AFM coupling strength with the increase in Fe-content as the ferromagnetic exchange in the martensite phase was observed to be enhanced with the increase in Fe-content.

From the dM/dT curves upon heating and cooling shown in the insets, thermal hysteresis of the martensitic transitions were found to increase with increase in Fe-content which is in good agreement with the DSC results. These observations are similar to that reported in NiMnFeGa alloys which convey that the presence of Fe atoms in the NiMnGa systems increases the energy required for phase boundary motion which might result in a decrease of the thermal elasticity in martensitic

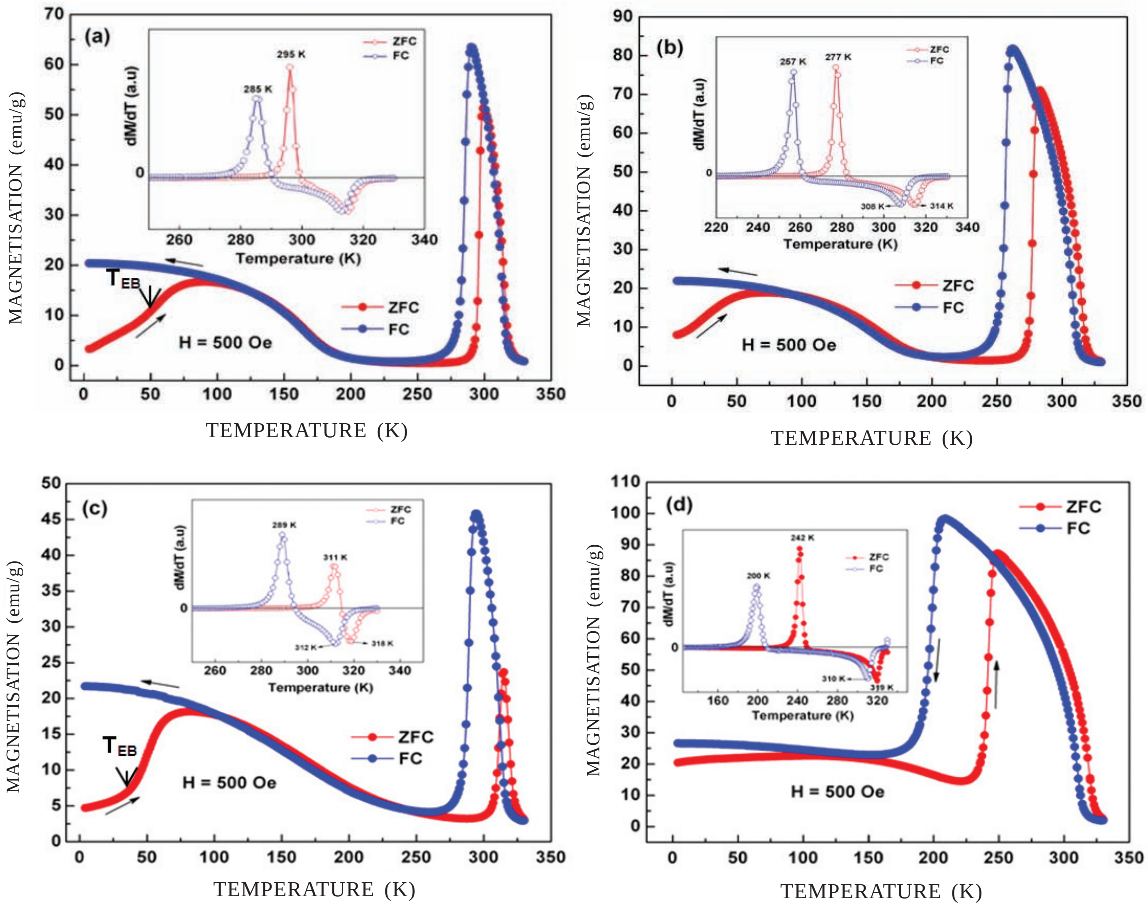

Figure 3. ZFC and FC thermomagnetic curves of $Ni_{47}Mn_{40-x}Fe_xIn_{13}$ ribbons with (a) x = 1, (b) x = 2, (c) x = 3 and (d) x = 5 for an applied field of 0.05 T (500 Oe). Inset shows the dM/dT curves upon heating (red) and cooling (blue).

transformation[26]. In the case of a Curie transition, the dM/dT curves should overlap upon heating and cooling indicating no thermal hysteresis as it is a second order transition. But, in this alloy series, the cyclic dM/dT curves of x = 2, 3, and 5 ribbons have also shown small thermal hysteresis (referring to the negative dM/dT peaks) in the vicinity of their respective Curie transitions unlike that observed in the case of second order transitions. This can be attributed to the presence of martensitic transition in the vicinity of Curie transition (T_C^A) that is giving rise to the observed thermal hysteresis.

3.3 Exchange Bias

A shift in field cooled M-H curve along field axis is the characteristic behaviour of exchange bias phenomena. It was verified by measuring the ZFC and FC hysteresis loops of x = 1 ribbon at different temperatures (a) 5 K, (b) 30 K, (c) 50 K, (d) 70 K (Fig. 4) in the field range of -2 T to 2 T. However, for better clarity the loops were shown from -0.2 T to 0.2 T in Fig. 4. It was found that, the FC loop shifts to negative field from origin up to a temperature of 50 K and at 70 K the shift was absent. On the other hand, the ZFC loop did not show any shift for all the set temperatures in the range of 5 K - 70 K. It implies that the EB phenomenon present for temperatures below T_{EB} (~ 55 K) for the x = 1 ribbon. The coercivity (H_C) and EB field (H_E) values were determined from the FC hysteresis loops using $H_E = -(H_1+H_2)/2$ and coercivity $H_c = |H_1-H_2|/2$ where the H_1 and H_2 are the negative field and positive field at which the magnetisation equals to zero. On increasing the temperature the H_E (Fig. 5) is found to decrease linearly and become zero as the temperature approaches T_{EB} (~ 70 K), whereas the H_C increases up to a maximum value of 260 Oe at 70 K and after that it decreases with further increase in temperature. The disappearance of H_E above T_{EB} confirms that the EB phenomenon exists only below T_{EB}. The H_E and H_C values are 175 Oe and 55 Oe at 10 K, respectively. The H_C curve presents a maximum value of 260 Oe at 70 K. Such dependencies of H_E and H_C are typical for EB systems[27]. The weakening of AFM-FM coupling due to the decrease of AFM region size on increasing temperature could be the reason for the observed trend in H_E and H_C. The evidence of EB results in $Ni_{47}Mn_{40-x}Fe_xIn_{13}$ ribbons signifies the existence of AFM-FM interactions. However, the other methods such as neutron diffractions studies are required to probe these kinds of magnetic structures in further detail.

3.4 Effect of Magnetic Field on the Martensitic Transitions

To understand the effect of magnetic field on structural and magnetic transitions, the thermomagnetic curves of $Ni_{47}Mn_{40-x}Fe_xIn_{13}$ ribbons were measured in a high magnetic field of 5 T

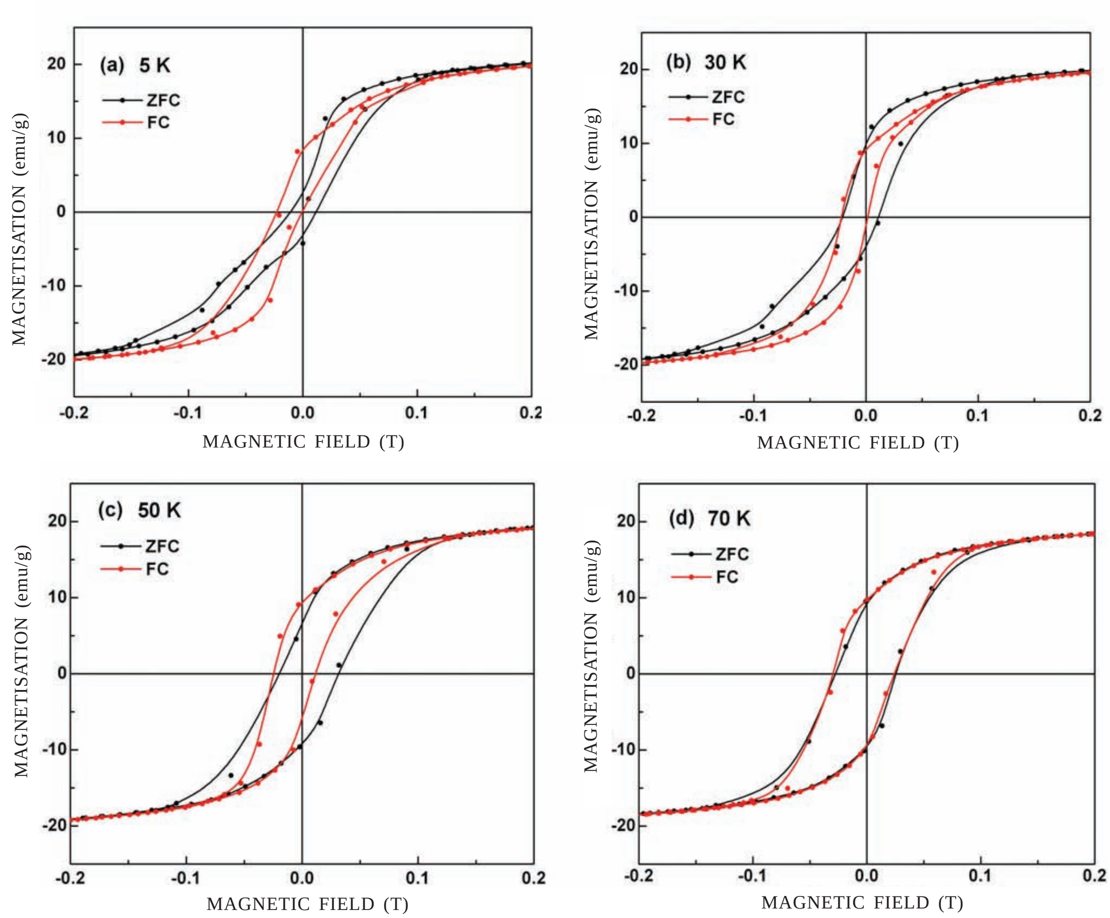

Figure 4. The ZFC and FC hysteresis loops of $Ni_{47}Mn_{40-x}Fe_xIn_{13}$ ribbon (x = 1) (a) 10 K, (b) 30 K, (c) 50 K, (d) 70 K. The sample is cooled in a field of 5 T for FC loops. The loops are displayed from -0.2 to 0.2 T for clear visualisation of the loop shift.

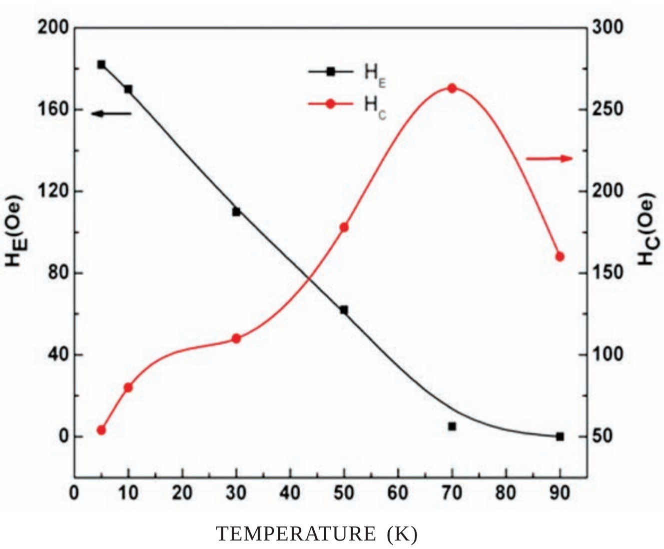

Figure 5. Exchange bias field (H_E) and coercivity (H_C) as a function of temperature in $Ni_{47}Mn_{40-x}Fe_xIn_{13}$ ribbon (x = 1).

upon heating and cooling in the temperature range of 5 K - 330 K (Fig. 6). The features in the high field curves are also similar to those shown in low field data (Fig. 3), but exhibit broad transformations. These ribbons show a shift in martensite start temperatures M_s [$\Delta T = M_s(5\ T) - M_s(0.05\ T)$] towards lower temperatures as the applied magnetic field increases (Table 2).

Table 2. Martensite start temperatures (M_s) at 50 mT and 5 T fields and the shift in the martensite start M_s (ΔT) both experimental and calculated from Clausius-Claypeyron relation

x	M_s (50 mT) (K)	M_s (5 T) (K)	ΔT (K) {Expt.}	ΔT (K) {C-C equ.}
1	290	275	15	15.1
2	262	237	25	24.3
3	294	281	13	13.6
5	208	142	66	20

For the x = 1, 2, 3 and 5 ribbons, the M_s values shifted by 15 K, 25 K, 13 K, and 66 K respectively, for a field change of 4.95 T. The x = 5 ribbon showed a maximum rate of change of M_s with respect to field (11.2 K/ T) in this alloy series. The change of M_s with field signifies a field induced transition from the martensite to the austenite phase. The lowering of the martensitic transition in these ribbons implies that the magnetic field favors the formation of the austenitic phase. Conversely, in Ni-Mn-Ga alloys, the M_s was reported to shift to higher temperatures with increasing magnetic field[28]. This kind of behaviour is due to the fact that the saturation magnetisation of the martensitic phase is larger than that of the austenite in Ni–Mn–Ga in contrast to that of Ni–Mn–X (X = Sn, In, Sb), wherein the martensitic phase has a lower magnetisation than

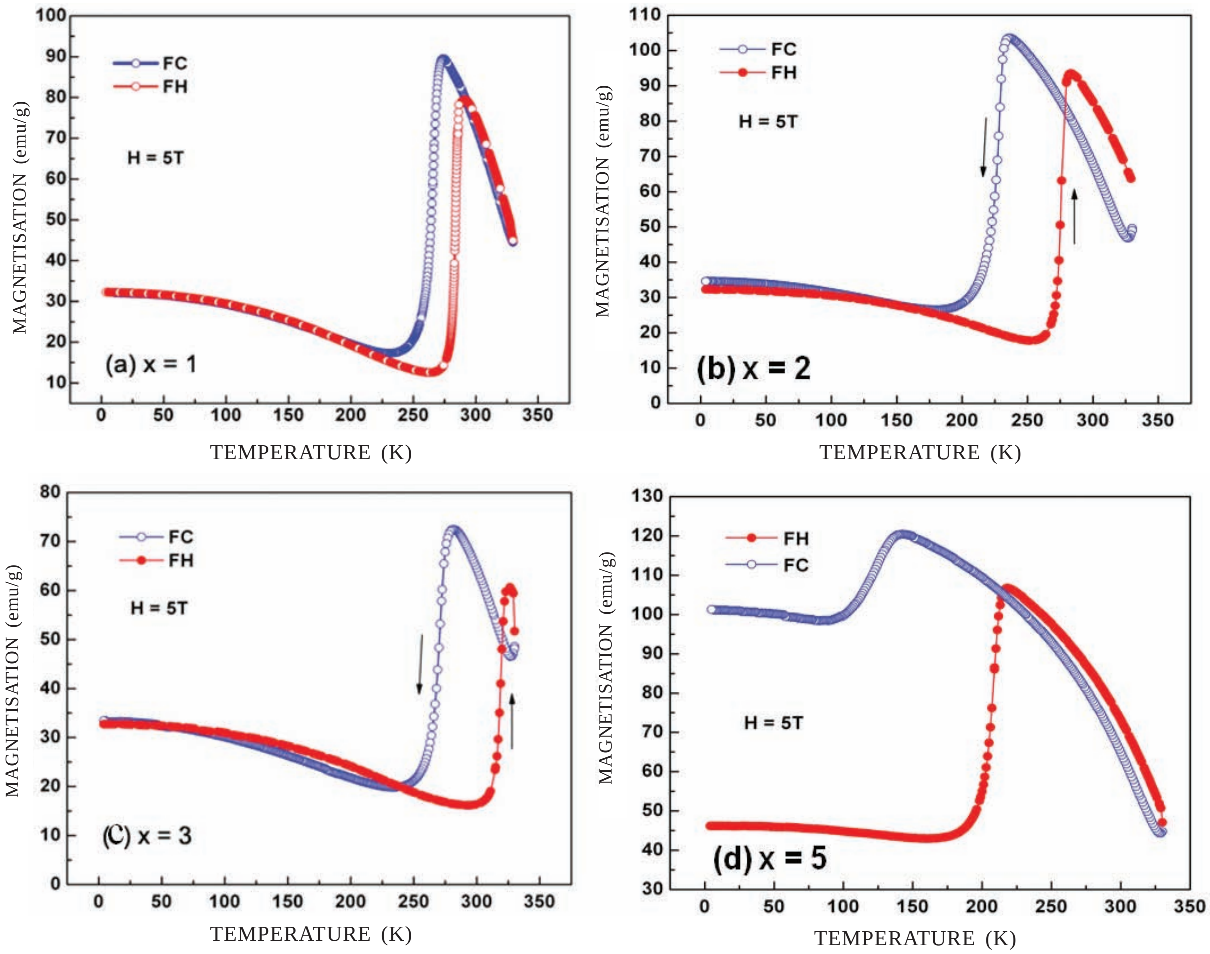

Figure 6. Field cooled (FC) and field heated (FH) M(T) curves of $Ni_{47}Mn_{40-x}Fe_xIn_{13}$ ribbons with (a) x = 1, (b) x = 2, (c) x = 3 and (d) x = 5 for an applied field of 5 T.

the austenitic phase. The M_s shift (ΔT) induced by magnetic field change ΔH can also be calculated approximately by Clausius-Claypeyron relation [C-C relation]

$$\Delta T = \left(\frac{\Delta M}{\Delta S}\right)\Delta H$$

where ΔM and ΔS are the differences in magnetisation and thermal entropy between the austenite and martensite phases. The ΔS values of the ribbons are calculated from the enthalpy data obtained from DSC. In the case of x = 2 ribbon where two transitions are observed, the sum of the two thermal entropies at those transitions have been taken into account for calculation. The experimental and the theoretical values (C-C equation) of the shift in the M_s are comparable in the case of x = 1, 2 and 3 ribbons. In the case of x = 5 ribbon, the M_s values do not match because some of the volume fraction of the austenite phase is retained even at low temperatures (up to 4 K) in the presence of high field. Hence, the C-C equation is valid only when the phase transformation from austenite to martensite phase is complete.

A kinetic arrest phenomenon has been reported in Ni-Mn-In alloys[29,30]. In this phenomenon, the MT is interrupted at certain temperatures during magnetic field cooling and does not proceed with further cooling. The parent (austenite) phase remains down to low temperatures. From the FC and FH $M(T)$ curves of the x = 5 ribbon, it can be said that this ribbon displays kinetic arrest phenomenon because of which the transformation to martensite upon cooling was not complete. Although such a peculiar behaviour of entropy change would be associated with the magnetic contribution to the Gibbs energy of the parent phase, the origin is still under discussion.

3.5 Magnetic Isotherms and Magnetocaloric Effect

The isothermal magnetic entropy change (ΔS_M) as a function of temperature was studied for the $Ni_{47}Mn_{40-x}Fe_xIn_{13}$ ribbons by measuring the isothermal magnetisation curves at different temperatures in the vicinity of their respective martensitic transformations. The isothermal magnetisation curves were measured in both increasing (0-5 T) and decreasing (5-0 T) fields. The isotherms of the ribbons were measured at a temperature interval of 2 K around T_M. The typical cyclic M-H loops of the x = 1 and 3 ribbons (Fig. 7) exhibit magnetic hysteresis around their respective T_M due to the magnetic field induced reverse martensitic transformations. The magnetisation values were found to increase with increasing temperature in the ranges of 276 K - 294 K and 292 K - 304 K for the x = 1 and 3 ribbons respectively, in the austenite region and upon further increase in temperature magnetisation decreases in both the cases. This is due to the transformation of martensite phase in to austenite phase. Similar behaviour was observed in the

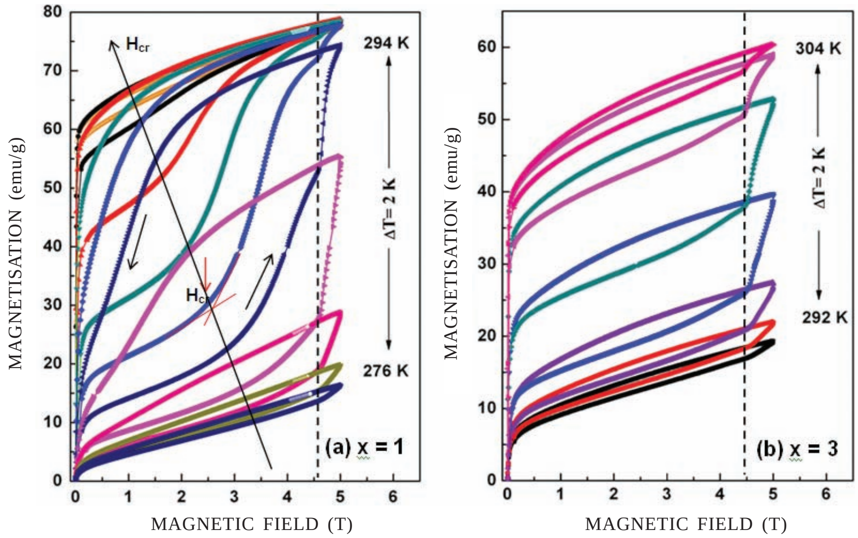

Figure 7. Isothermal magnetisation curves for $Ni_{47}Mn_{40-x}Fe_xIn_{13}$ ribbons in the vicinity of their martensitic transitions (a) x=1 in the temperature range of 276-294 K (b) x=3 in the temperature range of 292-304 K.

x = 2 and 5 ribbons as well in the vicinity of their martensitic transitions. The critical field (H_{cr}) defining the transition point is determined as the crossing point of the linear portion of the curves. This behaviour is attributed to the onset of magnetic field induced structural transition (FIST) from martensite to austenite phase. The x = 1 and 2 ribbons have shown the presence of strong FIST, whereas, the x = 3 ribbon showed feeble FIST and in the case of x = 5, the FIST was observed to be moderate. In the case of x = 1, 2, and 5 ribbons, the shift in H_{cr} to lower fields (shown by solid line with arrow) with increasing temperature could be observed. This is because the martensite to austenite phase transition is driven by both field and temperature, the critical field required to drive the structural transition at higher temperature in the magneto-structural transition regime is smaller. The absence of a strong FIST in the x = 3 ribbon suggests that the critical field required to induce a strong FIST is more than 5 T. Temperature alone is enough for driving the structural transition and in addition to that if magnetic field is applied, it becomes much easier to induce a strong FIST at lower critical fields. Apart from H_{cr}, there is another slope change observed in the M-H curves upon increasing fields (shown by dotted line) around 4.5 T. This can be explained as follows: the maximum applied field (here 5 T) is not enough to reach saturation point and upon decreasing the field, the M-H curve will reverse with higher magnetisation value. The M-H curve upon increasing field is only getting connected to the M-H curve upon decreasing field resulting in the slope change.

The temperature dependence of ΔS_M calculated in the decreasing field for $Ni_{47}Mn_{40-x}Fe_xIn_{13}$ ribbons are shown in Fig. 6. A maximum positive ΔS_M value (IMCE) of 50 J/kg K has been achieved both in the x = 1 and 2 ribbons, however at different temperatures ~ 282 K and 255 K respectively for a ΔH of 5 T. These values are more than that reported in $Ni_{50-y}Fe_yMn_{37}In_{13}$ (y = 1, 3) alloys[31]. On the other hand, maximum positive ΔS_M values of ~35 J/kg K at 298 K and ~25 J/kg K at 208 K have been obtained in the x = 3 and 5 ribbons respectively. The refrigerant capacities (RC) of the ribbons have also been summarised in the Table 3.

The obtained large ΔS_M values around T_M in the x = 1 and 2 ribbons is due to large change in the magnetisation values of

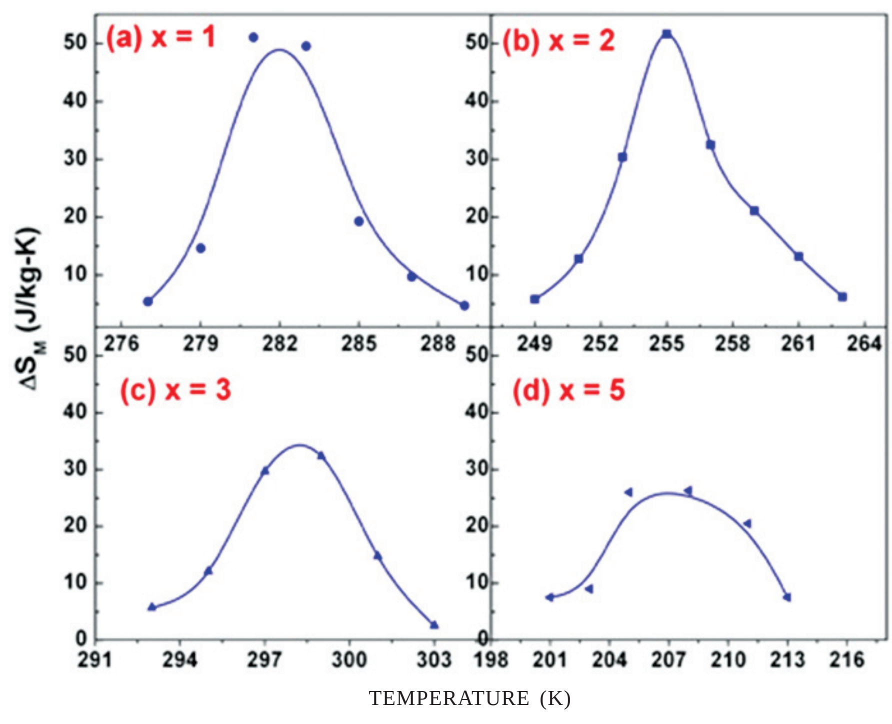

Figure 8. The temperature dependence of ΔS_M in $Ni_{47}Mn_{40-x}Fe_xIn_{13}$ ribbons measured on decreasing field (5-0 T). (a) x = 1, (b) x = 2, (c) x = 3 and (d) x = 5.

Table 3. Values of magnetic entropy change (ΔS_M), temperature at which IMCE attains maxima (T_{IMCE}^{max}) and refrigeration capacity (RC) in $Ni_{47}Mn_{40-x}Fe_xIn_{13}$ ribbons obtained on decreasing field in the vicinity of martensitic transitions

x	ΔS_M (J/kg K) (2-0 T)	ΔS_M (J/kg K) (5-0 T)	T_{IMCE}^{max} (K)	RC (J/kg) (5-0 T)	Hyst. Loss (J/kg)	Net RC (J/kg) (0-5 T)
1	16	50	282	227	110	117
2	15	50	255	204	116	88
3	12	32	298	140	65	75
5	9	25	208	202	142	60

the martensite and austenite phases in a narrow temperature interval arising due to a strong field induced structural transition compared to those observed in x = 3 and 5 ribbons. The ΔS_M values decrease with increase in Fe-content suggesting that Fe may aid in suppressing the field induced structural transition. The refrigerant capacity (RC) values for the $Ni_{47}Mn_{40-x}Fe_xIn_{13}$ ribbons calculated from the integration of ΔS_M over the full width at half maxima are given in Table 3. The RC values are estimated to be 227 J/kg, 204 J/kg, 140 J/kg, and 202 J/kg on decreasing fields for x = 1, 2, 3, and 5 ribbons, respectively. The estimated average hysteresis losses for the ribbons at temperatures where ΔS_M values attain their respective maxima are also given in the Table 3. Therefore, the net RC values of the ribbons obtained by subtracting the average hysteresis losses from their RC values were 117 J/kg, 88 J/kg, 75 J/kg, and 60 J/kg for x = 1, 2, 3, and 5, respectively.

4. SUMMARY

Structure, thermo-magnetic behaviour and magnetocaloric effect have been studied in $Ni_{47}Mn_{40-x}Fe_xIn_{13}$ ribbons. All the compositions (x = 1 to 5) have shown the presence of austenite phase at RT. It was found that the variation of martensitic transition (T_M) with the increase in Fe (x = 1 to 5) concentration was non-monotonic. This suggests that the exclusive dependence of martensitic transitions on e/a values is not universal and in some compositions (like in the present case) other factors are predominant. The presence of Fe did not have much influence on the T_C^A. The thermal hysteresis of the martensitic transition increased with the increase in Fe-content. The ribbons showed a shift in martensite start temperatures towards lower temperatures in the presence of high magnetic fields.

REFERENCES

1. Aksoy, S.; Acet, M.; Deen, P.P.; Manosa, L. & Planes, A. Magnetic correlations in martensitic Ni-Mn-based Heusler shape alloys: Neutron polarization analysis. *Phys. Rev. B.*, 2009, **79,** 212401. doi:10.1103/PhysRevB.79.212401
2. Planes; Manosa, L & Acet, M. Magnetocaloric effect and its relation to shape-memory properties in ferromagnetic Heusler alloys. *J. Phys.: Condensed Matter.*, 2009, **21,** 233201.
3. Sahoo, R.; Nayak, A.K.; Suresh, K.G. & Nigam, A.K. Effect of Fe substitution on the magnetic, transport, thermal and magnetocaloric properties in Ni-Mn-Fe-Sb Heusler alloys. *J. Appl. Phys.*, 2011, **109,** 123904. doi: 10.1063/1.3590398
4. Krenke, T.; Moya, X.; Aksoy, S.; Acet, M.; Entel, P.; Manosa, L.; Planes, A.; Alerman, Y.; Yucel, A.; Wassermann, E.F. Electronic aspects of the martensitic transition in Ni-Mn based Heusler alloys. *J. Magn. Magn. Mater.*, 2007, **310,** 2788. doi: 10.1016/j.jmmm.2006.10.1139
5. Dubenko, L.; Khan, M.; Pathak, A.K.; Gautam, B.R.; Stadler, S.; Ali, N. Magnetocaloric effect in Ni-Mn-X based Heusler alloys with X = Ga, Sb, In. *J. Magn. Magn. Mater.*, 2009, **321,** 754. doi: 10.1016/j.jmmm.2008.11.043
6. Rama Rao, N.V.; Gopalan, R.; Ch&rasekaran, V. & Suresh, K.G. Large low field inverse magnetocaloric effect near room temperature in Ni50-xMn37-xIn13 Heusler alloys. *Appl. Phys. A*, 2010, **99**, 265. doi: 10.1007/s00339-009-5517-3
7. Kainuma, R.; Imano, Y.; Ito, W.; Sutou, Y.; Morito, H.; Okamoto, S.; Kitakami, O.; Oikawa, K.; Fujita, A.; Kanomata, T. & Ishida, K. Magnetic field induced shape recovery by reverse phase transformation. *Nature*, 2006, **439**, 957. doi: 10.1038/nature04493
8. Rama Rao, N.V.; Gopalan, R.; Manivel Raja, M.; Ch&rasekaran, V. & Suresh, K.G. Mossbauer studies on structural ordering and magnetic properties of melt spun Ni-Fe-Ga ribbons. *Appl. Phys. Lett.*, 2008, **93,** 202503. doi: 10.1063/1.3028342
9. Liu, J.; Scheerbaum, N.; Hinz, D. & Gutfliesch, O. Martensitic transformation and magnetic properties in Ni-Fe-Ga-Co magnetic shape memory alloys. *Acta Mater.*, 2008, **56,** 3177. doi: 10.1016/j.actamat.2008.03.008
10. Zhao, X.G.; Hsieh, C.C.; Lai, J.H.; Cheng, X.J.; Chang, W.C.; Cui, W.B.; Liu, W. & Zhang, Z.D. Effects of annealing on magnetic entropy change and exchange bias behavior in melt spun Ni-Mn-In ribbons. *Scripta Mater.*, 2010, **63,** 250. doi: 10.1016/j.scriptamat.2010.03.067
11. Ma, Y.; Jiang, C.; Xu, H.; Wang, C. & Liu, X. Study of $Ni_{50+x}Mn_{25}Ga_{25-x}$ (x = 2-11) as high temperature shape memory alloys. *Acta Mater.*, 2007, **55,** 1533. doi: 10.1016/j.actamat.2006.10.014
12. Raj kumar, D.M.; Sridhar Rao, D.V.; Rama Rao, N.V.; Singh, R.K.; Manivel Raja, M. & Suresh, K.G. In-situ phase transformation studies of $Ni_{48}Mn_{39}In_{13}$ melt-spun ribbons. *Intermetallics*, 2012, **25,** 126.
13. Oikawa, K.; Ito W.; Imano Y.; Sutou Y.; Kainuma R.; Ishida K.; Okamoto S.; Kitakami O & Kanomata T. Effect of magnetic field transition of $Ni_{46}Mn_{41}In_{13}$ Heusler alloy. *Appl. Phys. Lett.*, 2006, **88,** 122507. doi: 10.1063/1.2187414
14. Pathak, A.K.; Khan, M.; Dubenko, I.; Stadler, S & Ali, N.

Large magnetic entropy change in $Ni_{50}Mn_{50-x}In_x$ Heusler alloys. *Appl. Phys. Lett.*, 2007, **90,** 262504.
doi: 10.1063/1.2752720

15. Liu, J.; Woodcock, T.G.; Scheerbaum, N. & Gutfleisch, O. Influence of annealing on magnetic field induced structural transformation and magnetocaloric effect in Ni-Mn-In-Co ribbons. *Acta Materialia.*, 2009, **57,** 4911.
doi: 10.1016/j.actamat.2009.06.054
16. Cai, W.; Feng, Y.; Sui, J.H.; Gao, Z.Y. & Dong, G.F. Microstructure and martensitic transformation behavior of the $Ni_{50}Mn_{36}In_{14}$ melt spun ribbons. *Scripta Materialia.*, 2008, **58,** 830.
doi: 10.1016/j.scriptamat.2007.12.035
17. Krenke, T.; Acet, M.; Wassermann, E.F.; Moya, X.; Manosa, L. & Planes, A. Ferromagnetism in the austenite and martensite states of Ni-Mn-In alloys. *Phys. Rev. B.*, 2006, **73,** 174413.
doi: 10.1103/PhysRevB.73.174413
18. Raj kumar, D.M.; Rama Rao, N.V.; Manivel Raja, M.; Sridhar Rao, D.V.; Srinivas, M.; Esakki Muthu, S.; Arumugam, S. & Suresh, K.G. Structure, magneto-structural transitions and magnetocaloric properties in $Ni_{50-x}Mn_{37+x}In_{13}$ melt spun ribbons. *J. Magn. Mag. Mater.*, 2012, **324,** 26.
19. Feng, Y.; Sui, J.H.; Gao, Z.Y.; Zhang, J.; Cai, W. Investigation on martensitic transformation behavior, microstructures and mechanical properties of Fe-doped Ni–Mn–In alloys. *Mater. Sci. Engg. A.*, 2009, **507,** 174.
doi: 10.1016/j.msea.2008.12.003
20. Chatterjee, S.; Giri S.; Majumdar S.; De, S.K. & Koledov, V.V. Effect of Sn doping on the martensitic and pre-martensitic transitions in Ni_2MnGa. *J. Magn. Magn. Mater.*, 2012, **324,** 1891.
21. Jiang, C.; Muhammad Y.; Deng L.; Wu W. & Xu H. Composition dependence on the martensitic structures of the Mn-rich NiMnGa alloys. *Acta Mater.*, 2004, **52,** 2779.
doi: 10.1016/j.actamat.2004.02.024
22. Khovailo, V.V.; Buchelnikov, V.D.; Kainuma, R.; Koledov V.V.; Ohtsuka, M.; Shavrov V.G.; Takagi, T.; Taskaev, S.V & Vasilev, A.N. Phase transition in $Ni_{2+x}Mn_{1-x}Ga$ with a high Ni excess. Phys. Rev. B ., 2005, **72,** 224408.
23. Chernenko, V.A. Compositional instability of β-phase in Ni-Mn-Ga alloys. *Scripta Mater.*, 1999, **40,** 523.
doi: 10.1016/S1359-6462(98)00494-1
24. MacLaren, J.M. Role of alloying on the shape memory effect in Ni_2MnGa. *J. Appl. Phys.*, 2002, **91,** 7801.
doi: 10.1063/1.1449440
25. Chatterjee, S.; Giri, S.; Majumdar, S.; De, S.K. & Koledov, V.V. Giant magneto-caloric effect near room temperature in Ni–Mn–Sn–Ga alloys. *J. Alloys Compds.*, 2010, **503,** 273.
doi: 10.1016/j.jallcom.2010.05.026
26. Liu, Z.H.; Zhang, M.; Wang, W.Q.; Wang, W.H.; Chen, J.L.; Wu, G.H.; Meng, F.B.; Liu, H.Y.; Liu, B.D.; Qu, J.P. & Li, Y.X. Magnetic properties and martensitic transformation in quaternary Heusler alloy of NiMnFeGa. *J. Appl. Phys.*, 2002, **92,** 5006.
doi: 10.1063/1.1511293
27. Khan, M.; Dubenko, I.; Stadler, S.; Ali, N. Exchange Bias Behavior in Ni–Mn–Sb Heusler Alloys. *Appl. Phys. Lett.*, 2007, **91,** 072510.
doi: 10.1063/1.2772233
28. Gama, S.; Coelho, A.A.; de Campos, A.; Carvalho, A.M.G.; Gandra, F.C.G.; Von Ranke, P.J & de Oliveira, N.A. Pressure-induced colossal magnetocaloric effect in MnAs. *Phys. Rev. Lett.* 2004, **93,** 237202.
doi: 10.1103/PhysRevLett.93.237202
29. Umetsu, R.Y.; Ito, W.; Ito, K.; Koyama, K.; Fujita, A.; Oikawa, K.; Watanable, K.; Kanomata, T.; Kainuma, R.; Ishida, K. Anomaly in entropy change between parent and martensite phases in the $Ni_{50}Mn_{34}In_{16}$ Heusler alloy. *Scripta Mater.*, 2009, **60,** 25.
doi: 10.1016/j.scriptamat.2008.08.022
30. Sharma, V.K.; Chattopadhyay, M.K. & Roy, S.B. Kinetic arrest of first order austenite to martensite phase transition in $Ni_{50}Mn_{34}In_{16}$ dc magnetization studies. *Phys. Rev. B.*, 2007, **76,** 140401(R).
doi: 10.1103/PhysRevB.76.140401
31. Krenke, T.; Duman, E.; Acet, M.; Moya, X.; Manosa, L. & Planes, A. Effect of Co and Fe on the inverse magnetocaloric properties of Ni-Mn-Sn. *J. Appl. Phys.*, 2007, **102,** 033903.
doi: 10.1063/1.2761853

ACKNOWLEDGEMENTS

This work was supported by Defence Research and Development Organisation, India. We thank the Director DMRL, and Dr S.V. Kamat, Group Head AMG, for their support and encouragement.

CONTRIBUTORS

Dr. D M Raj Kumar received M Tech (Solid State Technology) from IIT Kharagpur and PhD (Physics) from IIT Bombay. He is working as Scientist in the advanced magnetics group, DMRL, Hyderabad. His area of research interests include: Rare-earth permanent magnets and magnetocaloric materials.
In the current study, his contribution: Preparation of melt spun ribbons, structural characterization and complete analysis

Dr N.V. Rama Rao received MTech (Solid State Materials) from IIT Delhi and PhD (Physics) from IIT Bombay. He is working as Scientist in the Advanced Magnetics Group, DMRL, Hyderabad. His area of research interests include: Rare-earth permanent magnets, rare-earth free/lean permanent magnets and magnetocaloric materials.
In the current study, his contribution: Structural phase transitions through calorimetry and analysis.

Dr S. Esakki Muthu received PhD from Bharathidasan University, Centre for high pressure Research School of Physics, Trichy and currently, Currently, He is working as a Post-Doctoral fellow in CEFIPRA INAC/IMPEC, France.
In the current study, his contribution: Magnetic phase transitions and measurement of isotherms.

Prof. S. Arumugam is working as a Professor and Coordinator for Centre for high pressure research school of Physics, Bharathidasan University, Trichy. Research areas: Magnetism and magnetic materials, high pressure studies, magneto-transport properties and magnetocaloric materials.
In the current study, his contribution: Exchange bias measurements and magneto-structural phase transitions.

Dr M. Manivel Raja received PhD (Physics) from University of Madras. He is working as Scientist in the Advanced Magnetics Group, DMRL, Hyderabad. Research areas: Magnetism and magnetic materials, mossbauer spectroscopy, magnetic thin films, magnetic sensors and spintronics.
In the current study, his contribution: Ideas, analysis on magneto-structural transitions and magnetocaloric effect.

Prof. K.G. Suresh received PhD (Physics) from IIT Chennai. He is working as a Professor in Department of Physics, IIT Bombay. Research areas: Magnetism and magnetic materials, low temperature phenomena, magnetic thin films, rare-earth transition metal alloys and Spintronics.
In the current study, his contribution: Field cooled measurements, ideas, analysis on magneto-structural transitions and magnetocaloric effect.